

Numerical Analysis of Air Supply Alternatives for Forced-Air Precooling of Agricultural Produce

Grid independence study

A standard grid independence study was conducted using Grid Convergence Index (GCI) approach. GCI value was calculated as follows:

$$\epsilon = \frac{f_1 - f_2}{f_1} \quad (S1)$$

$$r = \sqrt[3]{\left(\frac{N_{fine}}{N_{coarse}}\right)} \quad (S2)$$

$$GCI = \frac{3|\epsilon|}{(r^p - 1)} \quad (S3)$$

where ϵ is a relative error indicator, f_1 is the variable value at a designated point with relatively fine grid, f_2 is the variable value at the same point with coarse grid. The mesh refinement ratio r is calculated using the total number of cells of a fine mesh (N_{fine}) and a coarse mesh (N_{coarse}). GCI value was calculated using ϵ and r , with p represents the numerical scheme order of accuracy and is 2 for second order scheme in this study.

Also, we picked three points P1, P2, and P3 as monitoring locations to assess GCI changes, whose coordinates were shown in Table S1. Three mesh files of control model were created with 0.8, 1.5 and 4 million cells respectively. The GCI value was calculated and compared at P1, P2, and P3 in terms of air speeds, which showed a declining trend when r increased from 1.22 to 1.38. Hence, GCI decreased with finer mesh at the same numerical accuracy order, which indicated the mesh refining approach was on the right track. However, the finest mesh scale (4 million) demanded considerable computational resources and costed excessive time to complete the calculation. Given the sufficient accuracy that has been improved by the median scale and its

reasonable computational costs, the size of 1.5 million was chosen beyond the 4 million set to proceed further modelling.

Table S1. GCI values calculated by corresponding mesh refinement ratios using the second order scheme.

Points	Location			GCI value	
	x	y	z	$r = 1.38$	$r = 1.22$
P1	-0.5	1.5	-1.5	226.60%	331.50%
P2	0.5	1.5	-1.5	541.09%	938.88%
P3	0	2	-1.5	4.02%	55.29%

Field measurement and model validation study

To validate CFD model more efficiently, we further simplified the control model by merely modeling the empty storage room. An electric heater (SINFUN, Ningbo, China) was deployed as the only heating source and was modeled accordingly. The dimensions of the heater are 570x308x650 mm with the maximum power of 2200 W. The heater was covered by foil and was placed in the middle of the room facing the evaporator unit. Based on field measurement, the evaporator was operated at full speed with a mass flow rate of 2.36 kg/s, and the temperature and water vapor mass fraction of incoming cooling air was 8.7 °C and 0.00525, respectively.

The corresponding CFD model has the same computational domain size but with a smaller size of mesh compared to the control model, which is 77,935 cells (Fig. S1). Identical boundary condition settings were defined except for the temperature and mass fraction of H₂O for inlet. In addition, the heater was modeled as a solid block made of aluminum with a heating rate of 19,279 W/m³. A steady-state simulation was conducted with 2500 iterations to ensure the solution has converged.

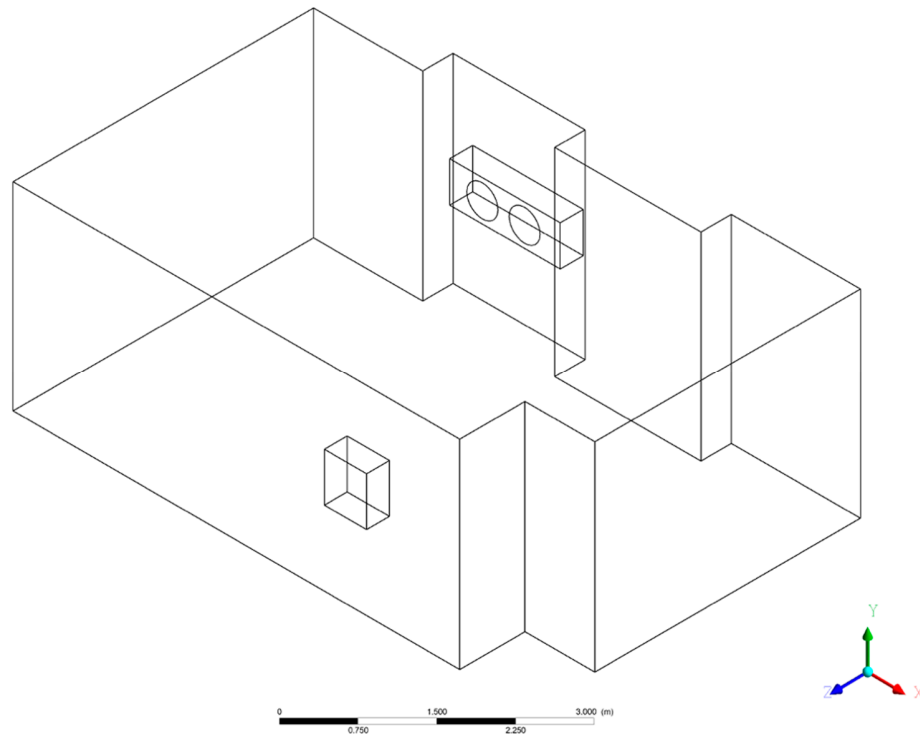


Figure S1. Computational domain of the CFD model for validation.

Temperature, relative humidity, and air velocity measurements were performed at 16 locations in total. Specific locations of the 16 spots were listed in Table S2. Air temperature and relative humidity were measured and recorded using a Testo 480 digital meter with IAQ probe (Testo, Lenzkirch, Germany). The accuracy of IAQ probe is ± 0.3 °C for temperature and $\pm 2\%$ for relative humidity. Air speeds were measured using a Testo 0635-1543 hot wire anemometer (Testo, Lenzkirch, Germany) that has an accuracy of $\pm 4\%$ of reading and ± 0.03 m/s. The sampling rate is one reading per second. For temperature and relative humidity, the final readings were used when both parameters became stable. For air velocity measurement, the anemometer can only capture the velocity in one direction. Therefore, the anemometer was placed vertically with a tripod to measure horizontal air speeds that were considered as major air movements driven by the evaporator. Since air velocity reads fluctuate more or less even when indoor climate becomes stable, an average of 30 readings at each spot is used to represent the corresponding mean of air

speed. All the measured values were used for comparison and statistical analysis with prediction data generated by CFD simulation.

Table S2. Field measurement versus prediction data at 16 locations.

ID	Location			Static Temperature [K]		Velocity w [m s ⁻¹]		Relative Humidity RH [%]	
	X (m)	Y (m)	Z (m)	Measurement	Prediction	Measurement	Prediction	Measurement	Prediction
P1	0.00	0.77	-1.25	285.90	283.93	0.08	0.09	67.10	66.16
P2	-0.29	0.77	-1.25	286.60	285.49	0.13	0.14	55.80	59.36
P3	0.00	1.35	-1.25	283.10	282.91	0.11	0.12	67.20	70.54
P4	-0.29	1.35	-1.25	283.40	283.22	0.14	0.17	66.00	67.68
P5	0.29	1.35	-1.25	283.50	282.63	0.01	0.09	65.30	65.62
P6	-0.47	1.01	-1.03	283.60	285.89	0.15	0.20	69.30	64.57
P7	-0.47	1.35	-1.03	283.10	284.22	0.17	0.22	69.20	66.09
P8	-0.29	1.35	-0.98	282.80	284.49	0.13	0.27	70.70	68.24
P9	0.00	1.35	-0.87	282.50	284.07	0.14	0.28	70.80	68.00
P10	0.29	1.35	-0.87	282.60	282.86	0.15	0.17	73.90	68.71
P11	0.44	1.35	-1.04	282.50	282.52	0.17	0.16	71.90	67.89
P12	0.44	1.02	-1.04	282.60	282.39	0.21	0.23	71.00	66.42
P13	0.44	0.78	-1.04	282.70	282.56	0.19	0.26	71.00	67.20
P14	0.44	0.78	-1.11	282.90	282.48	0.19	0.21	70.80	72.78
P15	0.44	1.02	-1.11	282.90	282.37	0.20	0.19	69.80	73.04
P16	0.44	1.36	-1.11	282.80	282.52	0.18	0.15	85.30	72.43

In total, 5 evaluation parameters were used to assess the alignment between measurement and prediction data, which included fractional bias fractional bias (*FB*), geometric mean bias (*MG*), geometric mean-variance (*VG*), fraction within a factor of two (*FAC2*), and normalized mean square error (*NMSE*). Those evaluation indexes were calculated using following equations:

$$FB = 2 \frac{\bar{X}_m - \bar{X}_p}{\bar{X}_m + \bar{X}_p} \quad (S4)$$

$$MG = \exp \left[\ln \left(\frac{\bar{X}_m}{\bar{X}_p} \right) \right] \quad (S5)$$

$$VG = \exp \left[\ln \left(\frac{\bar{X}_m}{\bar{X}_p} \right)^2 \right] \quad (S6)$$

$$FAC2 = \frac{X_p}{X_m} \quad (S7)$$

$$NMSE = \frac{1}{N} \sum_{i=1}^N \left(\frac{X_m - X_p}{X_m \cdot X_p} \right)^2 \quad (S8)$$

where X_m stands for measured value of variables, X_p is predicted value of the variables, $\overline{X_m}$ and $\overline{X_p}$ are means of measured and predicted values with respect.